

A model for J/ψ absorption in hadronic matter

Ziwei Lin and C. M. Ko

*Cyclotron Institute and Physics Department, Texas A&M University, College Station, Texas
77843-3366*

Abstract

The cross sections of J/ψ absorption by π and ρ mesons are studied in a meson-exchange model that includes not only the pseudoscalar-pseudoscalar-vector-meson couplings but also the three-vector-meson and four-point couplings. We find that the J/ψ absorption cross sections, $\sigma_{\pi\psi}$ and $\sigma_{\rho\psi}$, are much larger than in a previous study where only pseudoscalar-pseudoscalar-vector-meson couplings were considered. Including form factors at vertices, their thermal averages $\langle\sigma_{\pi\psi}v\rangle$ and $\langle\sigma_{\rho\psi}v\rangle$ in a hadronic matter at a temperature of 150 MeV are found to have values of the order of 1 mb and 2 mb, respectively. PACS number(s): 25.75.-q, 14.40.Gx, 13.75.Lb

I. INTRODUCTION

A dense partonic system, often called the quark-gluon plasma (QGP), is expected to be formed in heavy ion collisions at the Relativistic Heavy Ion Collider (RHIC), which will soon start to operate at the Brookhaven National Laboratory. Of all experimental observables that are sensitive to the presence of the QGP, charmonium is among the most promising ones. In particular, the dissociation of charmoniums in the QGP due to the color screening would lead to a reduction of their production in relativistic heavy ion collisions. The suppression of charmonium production in these collisions has thus been proposed as a possible signature for the formation of the QGP [1]. Extensive experimental and theoretical efforts have since been devoted to study this phenomenon [2–6]. However, available experimental data on J/ψ suppression in colliding systems ranging from pA to S+U are consistent with the scenario that charmoniums are absorbed by target and projectile nucleons with a cross section of about 7 mb [5]. Only in recent data from the Pb+Pb collision at $P_{\text{lab}} = 158 \text{ GeV}/c$ in the NA50 experiment at CERN [4] is there a large additional J/ψ suppression in high E_T events, which requires the introduction of other absorption mechanisms. While there are suggestions that this anomalous suppression may be due to the formation of the QGP [7,8], other more conventional mechanisms based on J/ψ absorption by co-moving hadrons have also been proposed as a possible explanation [9,10]. Since the latter depends on the values of J/ψ absorption cross sections by hadrons, which are not known empirically, it is important to have a better knowledge on the interactions between charmonium states and co-moving hadrons in order to understand the nature of the observed anomalous charmonium suppression.

Knowledge on the J/ψ absorption cross sections by hadrons is also useful in estimating the contribution of J/ψ production from charm mesons in the hadronic matter formed in relativistic heavy ion collisions. Since the charm meson to J/ψ ratio in a proton-proton collision increases with energy, it has been shown that J/ψ production from a hadronic matter may not be negligible in heavy ion collisions at the Large Hadronic Collider energies [11]. To use J/ψ suppression as a signature for the formation of the QGP in these collisions thus requires the understanding of both J/ψ absorption and production in the hadronic matter.

Various approaches have been used in evaluating the charmonium absorption cross sections by hadrons. In one approach, the quark-exchange model has been used. An earlier study based on this model by Martins, Blaschke and Quack [12] showed that the J/ψ absorption cross section $\sigma_{\pi\psi}$ by pion had a peak value of about 7 mb at $E_{\text{kin}} \equiv \sqrt{s} - m_\pi - m_\psi \simeq 0.8$ GeV, but a recent study by Wong, Barnes and Swanson [13] gave a peak value of only $\sigma_{\pi\psi} \sim 1$ mb at the same E_{kin} region. In the perturbative QCD approach by Kharzeev and Satz [14] the dissociation of charmonium bound states by energetic gluons inside hadrons was studied. It has predicted that the dissociation cross section increases monotonously with E_{kin} and has a value of only about 0.1 mb around $E_{\text{kin}} \sim 0.8$ GeV. In the third approach, meson-exchange models based on hadronic effective Lagrangians have been used. Using pseudoscalar-pseudoscalar-vector-meson couplings (PPV couplings), Matinyan and Müller [15] found $\sigma_{\pi\psi} \simeq 0.3$ mb at $E_{\text{kin}} = 0.8$ GeV. In a more recent study, Haglin [16] included also the three-vector-meson couplings (VVV couplings) and four-point couplings, and much larger values of the J/ψ absorption cross sections were obtained. Large discrepancies in the magnitude of $\sigma_{\pi\psi}$ (as well as $\sigma_{\rho\psi}$) thus exist among the predictions from these three approaches, and further theoretical studies are needed. In the present study, we follow the approach of Haglin by using a meson-exchange model [16] but treat more completely the VVV and four-point couplings in the effective Lagrangian and also take into account of the effects of form factors at interaction vertices.

Our paper is organized as follows. In Sec. II we introduce the effective hadronic Lagrangian that we use to obtain the relevant interactions between J/ψ and hadrons. The cross sections for J/ψ absorption by π and ρ mesons are then evaluated. The amplitudes for the coherent sum of individual diagrams are checked to ensure that the current is conserved in the limit of zero vector meson masses. We then show in Sec. III the numerical results for the cross sections and their dependence on the form factors at interaction vertices. Finally, discussions and the summary are given in Sec. IV.

II. J/ψ ABSORPTION IN HADRONIC MATTER: ANALYTICAL RESULTS

A. The effective Lagrangian

The free Lagrangian for pseudoscalar and vector mesons in the limit of SU(4) invariance can be written as follows:

$$\mathcal{L}_0 = \text{Tr} \left(\partial_\mu P^\dagger \partial^\mu P \right) - \frac{1}{2} \text{Tr} \left(F_{\mu\nu}^\dagger F^{\mu\nu} \right) , \quad (1)$$

where $F_{\mu\nu} = \partial_\mu V_\nu - \partial_\nu V_\mu$, and P and V denote, respectively, the 4×4 pseudoscalar and vector meson matrices in SU(4) [17]. To obtain the couplings between pseudoscalar mesons and vector mesons, we introduce the minimal substitution,

$$\partial_\mu P \rightarrow \mathcal{D}_\mu P = \partial_\mu P - \frac{ig}{2} V_\mu P + \frac{ig}{2} P V_\mu , \quad (2)$$

$$F_{\mu\nu} \rightarrow \partial_\mu V_\nu - \partial_\nu V_\mu - \frac{ig}{2} [V_\mu, V_\nu] . \quad (3)$$

The effective Lagrangian involving the coupling between pseudoscalar and vector mesons is then

$$\begin{aligned} \mathcal{L} = \mathcal{L}_0 &+ \frac{ig}{2} \text{Tr} \left(\partial^\mu P [P^\dagger, V_\mu^\dagger] + \partial^\mu P^\dagger [P, V_\mu] \right) - \frac{g^2}{4} \text{Tr} \left([P^\dagger, V_\mu^\dagger] [P, V^\mu] \right) \\ &+ \frac{ig}{2} \text{Tr} \left(\partial^\mu V^\nu [V_\mu^\dagger, V_\nu^\dagger] + \partial_\mu V_\nu^\dagger [V^\mu, V^\nu] \right) + \frac{g^2}{8} \text{Tr} \left([V^\mu, V^\nu] [V_\mu^\dagger, V_\nu^\dagger] \right) . \end{aligned} \quad (4)$$

Hermiticity of P and V reduces this to

$$\begin{aligned} \mathcal{L} = \mathcal{L}_0 &+ ig \text{Tr} \left(\partial^\mu P [P, V_\mu] \right) - \frac{g^2}{4} \text{Tr} \left([P, V_\mu]^2 \right) \\ &+ ig \text{Tr} \left(\partial^\mu V^\nu [V_\mu, V_\nu] \right) + \frac{g^2}{8} \text{Tr} \left([V_\mu, V_\nu]^2 \right) . \end{aligned} \quad (5)$$

Since the SU(4) symmetry is explicitly broken by hadron masses, terms involving hadron masses are added to Eq.(5) using the experimentally determined values.

B. Effective Lagrangians relevant for J/ψ absorption

Expanding the Lagrangian in Eq.(5) explicitly in terms of the pseudoscalar meson and vector meson matrices [17], we obtain the following interaction Lagrangians that are relevant for the study of J/ψ absorption by π and ρ mesons:

$$\begin{aligned} \mathcal{L}_{\pi DD^*} &= ig_{\pi DD^*} D^{*\mu} \vec{\tau} \cdot \left(\bar{D} \partial_\mu \vec{\pi} - \partial_\mu \bar{D} \vec{\pi} \right) + \text{H.c.} , \\ \mathcal{L}_{\psi DD} &= ig_{\psi DD} \psi^\mu \left(D \partial_\mu \bar{D} - \partial_\mu D \bar{D} \right) , \\ \mathcal{L}_{\psi D^* D^*} &= ig_{\psi D^* D^*} \left[\psi^\mu \left(\partial_\mu D^{*\nu} \bar{D}_\nu^* - D^{*\nu} \partial_\mu \bar{D}_\nu^* \right) + \left(\partial_\mu \psi^\nu D_\nu^* - \psi^\nu \partial_\mu D_\nu^* \right) \bar{D}^{*\mu} \right. \\ &\quad \left. + D^{*\mu} \left(\psi^\nu \partial_\mu \bar{D}_\nu^* - \partial_\mu \psi^\nu \bar{D}_\nu^* \right) \right] , \\ \mathcal{L}_{\pi \psi DD^*} &= -g_{\pi \psi DD^*} \psi^\mu \left(D_\mu^* \vec{\tau} \bar{D} + D \vec{\tau} \bar{D}_\mu^* \right) \cdot \vec{\pi} , \\ \mathcal{L}_{\rho DD} &= ig_{\rho DD} \left(D \vec{\tau} \partial_\mu \bar{D} - \partial_\mu D \vec{\tau} \bar{D} \right) \cdot \vec{\rho}^\mu , \\ \mathcal{L}_{\rho \psi DD} &= g_{\rho \psi DD} \psi^\mu D \vec{\tau} \bar{D} \cdot \vec{\rho}_\mu , \\ \mathcal{L}_{\rho D^* D^*} &= ig_{\rho D^* D^*} \left[\left(\partial_\mu D^{*\nu} \vec{\tau} \bar{D}_\nu^* - D^{*\nu} \vec{\tau} \partial_\mu \bar{D}_\nu^* \right) \cdot \vec{\rho}^\mu + \left(D^{*\nu} \vec{\tau} \cdot \partial_\mu \vec{\rho}_\nu - \partial_\mu D^{*\nu} \vec{\tau} \cdot \vec{\rho}_\nu \right) \bar{D}^{*\mu} \right. \\ &\quad \left. + D^{*\mu} \left(\vec{\tau} \cdot \rho^\nu \partial_\mu \bar{D}_\nu^* - \vec{\tau} \cdot \partial_\mu \rho^\nu \bar{D}_\nu^* \right) \right] , \\ \mathcal{L}_{\rho \psi D^* D^*} &= g_{\rho \psi D^* D^*} \left(\psi^\nu D_\nu^* \vec{\tau} \bar{D}_\mu^* + \psi^\nu D_\mu^* \vec{\tau} \bar{D}_\nu^* - 2 \psi_\mu D^{*\nu} \vec{\tau} \bar{D}_\nu^* \right) \cdot \vec{\rho}^\mu . \end{aligned} \quad (6)$$

In the above, $\vec{\tau}$ are the Pauli matrices, $\vec{\pi}$ and $\vec{\rho}$ denote the pion and rho meson isospin triplets, respectively, while D and D^* denote the pseudoscalar charm meson and vector charm meson isospin doublets, respectively. We note that exact SU(4) symmetry would give the following relations among the coupling constants in the Lagrangian:

$$\begin{aligned} g_{\pi DD^*} &= g_{\rho DD} = g_{\rho D^* D^*} = \frac{g}{4}, \quad g_{\psi DD} = g_{\psi D^* D^*} = \frac{g}{\sqrt{6}}, \\ g_{\pi \psi DD^*} &= g_{\rho \psi D^* D^*} = \frac{g^2}{4\sqrt{6}}, \quad g_{\rho \psi DD} = \frac{g^2}{2\sqrt{6}}. \end{aligned} \quad (7)$$

C. J/ψ absorption cross sections

The above effective Lagrangian allows us to study the following processes for J/ψ absorption by π and ρ mesons:

$$\pi\psi \rightarrow D^* \bar{D}, \quad \pi\psi \rightarrow D \bar{D}^*, \quad \rho\psi \rightarrow D \bar{D}, \quad \rho\psi \rightarrow D^* \bar{D}^*. \quad (8)$$

Corresponding diagrams for these processes, except the process $\pi\psi \rightarrow D \bar{D}^*$ which has the same cross section as the process $\pi\psi \rightarrow D^* \bar{D}$, are shown in Fig. 1.

The full amplitude for the first process, $\pi\psi \rightarrow D^* \bar{D}$, without isospin factors and before summing and averaging over external spins (same for \mathcal{M}_2 and \mathcal{M}_3), is given by

$$\mathcal{M}_1 \equiv \mathcal{M}_1^{\nu\lambda} \epsilon_{2\nu} \epsilon_{3\lambda} = \left(\sum_{i=a,b,c} \mathcal{M}_{1i}^{\nu\lambda} \right) \epsilon_{2\nu} \epsilon_{3\lambda}, \quad (9)$$

with

$$\begin{aligned} \mathcal{M}_{1a}^{\nu\lambda} &= -g_{\pi DD^*} g_{\psi DD} (-2p_1 + p_3)^\lambda \left(\frac{1}{t - m_D^2} \right) (p_1 - p_3 + p_4)^\nu, \\ \mathcal{M}_{1b}^{\nu\lambda} &= g_{\pi DD^*} g_{\psi D^* D^*} (-p_1 - p_4)^\alpha \left(\frac{1}{u - m_{D^*}^2} \right) \left[g_{\alpha\beta} - \frac{(p_1 - p_4)_\alpha (p_1 - p_4)_\beta}{m_{D^*}^2} \right] \\ &\quad \times \left[(-p_2 - p_3)^\beta g^{\nu\lambda} + (-p_1 + p_2 + p_4)^\lambda g^{\beta\nu} + (p_1 + p_3 - p_4)^\nu g^{\beta\lambda} \right], \\ \mathcal{M}_{1c}^{\nu\lambda} &= -g_{\pi \psi DD^*} g^{\nu\lambda}. \end{aligned} \quad (10)$$

For the second process, $\rho\psi \rightarrow D \bar{D}$, the full amplitude is given by

$$\mathcal{M}_2 \equiv \mathcal{M}_2^{\mu\nu} \epsilon_{1\mu} \epsilon_{2\nu} = \left(\sum_{i=a,b,c} \mathcal{M}_{2i}^{\mu\nu} \right) \epsilon_{1\mu} \epsilon_{2\nu}, \quad (11)$$

with

$$\begin{aligned} \mathcal{M}_{2a}^{\mu\nu} &= -g_{\rho DD} g_{\psi DD} (p_1 - 2p_3)^\mu \left(\frac{1}{t - m_D^2} \right) (p_1 - p_3 + p_4)^\nu, \\ \mathcal{M}_{2b}^{\mu\nu} &= -g_{\rho DD} g_{\psi DD} (-p_1 + 2p_4)^\mu \left(\frac{1}{u - m_D^2} \right) (-p_1 - p_3 + p_4)^\nu, \\ \mathcal{M}_{2c}^{\mu\nu} &= g_{\rho \psi DD} g^{\mu\nu}. \end{aligned} \quad (12)$$

The full amplitude for the third process, $\rho\psi \rightarrow D^*\bar{D}^*$, is given by

$$\mathcal{M}_3 \equiv \mathcal{M}_3^{\mu\nu\lambda\omega} \epsilon_{1\mu}\epsilon_{2\nu}\epsilon_{3\lambda}\epsilon_{4\omega} = \left(\sum_{i=a,b,c} \mathcal{M}_{3i}^{\mu\nu\lambda\omega} \right) \epsilon_{1\mu}\epsilon_{2\nu}\epsilon_{3\lambda}\epsilon_{4\omega}, \quad (13)$$

with

$$\begin{aligned} \mathcal{M}_{3a}^{\mu\nu\lambda\omega} &= g_{\rho D^* D^*} g_{\psi D^* D^*} \left[(-p_1 - p_3)^\alpha g^{\mu\lambda} + 2 p_1^\lambda g^{\alpha\mu} + 2 p_3^\mu g^{\alpha\lambda} \right] \left(\frac{1}{t - m_{D^*}^2} \right) \\ &\quad \times \left[g_{\alpha\beta} - \frac{(p_1 - p_3)_\alpha (p_1 - p_3)_\beta}{m_{D^*}^2} \right] \left[-2 p_2^\omega g^{\beta\nu} + (p_2 + p_4)^\beta g^{\nu\omega} - 2 p_4^\nu g^{\beta\omega} \right], \\ \mathcal{M}_{3b}^{\mu\nu\lambda\omega} &= g_{\rho D^* D^*} g_{\psi D^* D^*} \left[-2 p_1^\omega g^{\alpha\mu} + (p_1 + p_4)^\alpha g^{\mu\omega} - 2 p_4^\mu g^{\alpha\omega} \right] \left(\frac{1}{u - m_{D^*}^2} \right) \\ &\quad \times \left[g_{\alpha\beta} - \frac{(p_1 - p_4)_\alpha (p_1 - p_4)_\beta}{m_{D^*}^2} \right] \left[(-p_2 - p_3)^\beta g^{\nu\lambda} + 2 p_2^\lambda g^{\beta\nu} + 2 p_3^\nu g^{\beta\lambda} \right], \\ \mathcal{M}_{3c}^{\mu\nu\lambda\omega} &= g_{\rho\psi D^* D^*} \left(g^{\mu\lambda} g^{\nu\omega} + g^{\mu\omega} g^{\nu\lambda} - 2 g^{\mu\nu} g^{\lambda\omega} \right). \end{aligned} \quad (14)$$

In the above, p_j denotes the momentum of particle number j . We choose the convention that particle numbers 1 and 2 represent initial-state mesons while particle numbers 3 and 4 represent final-state mesons on the left and right side of the diagrams shown in Fig. 1, respectively. The indices μ, ν, λ , and ω denote the polarization components of external particles while the indices α and β denote those of the exchanged mesons.

After averaging (summing) over initial (final) spins and including isospin factors, the cross sections for the three processes are given by

$$\frac{d\sigma_1}{dt} = \frac{1}{96\pi s p_{i,\text{cm}}^2} \mathcal{M}_1^{\nu\lambda} \mathcal{M}_1^{*\mu'\lambda'} \left(g_{\nu\nu'} - \frac{p_{2\nu} p_{2\nu'}}{m_2^2} \right) \left(g_{\lambda\lambda'} - \frac{p_{3\lambda} p_{3\lambda'}}{m_3^2} \right), \quad (15)$$

$$\frac{d\sigma_2}{dt} = \frac{1}{288\pi s p_{i,\text{cm}}^2} \mathcal{M}_2^{\mu\nu} \mathcal{M}_2^{*\mu'\nu'} \left(g_{\mu\mu'} - \frac{p_{1\mu} p_{1\mu'}}{m_1^2} \right) \left(g_{\nu\nu'} - \frac{p_{2\nu} p_{2\nu'}}{m_2^2} \right), \quad (16)$$

$$\begin{aligned} \frac{d\sigma_3}{dt} &= \frac{1}{288\pi s p_{i,\text{cm}}^2} \mathcal{M}_3^{\mu\nu\lambda\omega} \mathcal{M}_3^{*\mu'\nu'\lambda'\omega'} \left(g_{\mu\mu'} - \frac{p_{1\mu} p_{1\mu'}}{m_1^2} \right) \left(g_{\nu\nu'} - \frac{p_{2\nu} p_{2\nu'}}{m_2^2} \right) \\ &\quad \times \left(g_{\lambda\lambda'} - \frac{p_{3\lambda} p_{3\lambda'}}{m_3^2} \right) \left(g_{\omega\omega'} - \frac{p_{4\omega} p_{4\omega'}}{m_4^2} \right), \end{aligned} \quad (17)$$

with $s = (p_1 + p_2)^2$, and

$$p_{i,\text{cm}}^2 = \frac{[s - (m_1 + m_2)^2][s - (m_1 - m_2)^2]}{4s} \quad (18)$$

is the squared momentum of initial-state mesons in the center-of-momentum (CM) frame.

D. Current conservation

The effective Lagrangian in Eq.(5) is generated by the minimal substitution, which is equivalent to treating vector mesons as gauge particles. To preserve the gauge invariance in the limit of massless vector meson thus leads to both VVV and four-point couplings in the Lagrangian. The gauge invariance also results in current conservation, i.e.,

$$\mathcal{M}_n^{\lambda_k \dots \lambda_l} p_{j\lambda_j} = 0, \quad (19)$$

where the index λ_j denotes the external vector meson j in process n shown in Fig. 1. This then requires, e.g., $\mathcal{M}_1^{\nu\lambda} p_{3\lambda} = 0$, and $\mathcal{M}_3^{\mu\nu\lambda\omega} p_{2\nu} = 0$. We have explicitly checked that the amplitudes given in Eqs.(9)-(14) all satisfy the requirement of current conservation.

III. J/ψ ABSORPTION IN HADRONIC MATTER: NUMERICAL RESULTS

For the three-point coupling constants, we use the following empirical values [15]:

$$g_{\pi DD^*} = 4.4, \quad g_{\rho DD} = g_{\rho D^* D^*} = 2.8, \quad g_{\psi DD} = g_{\psi D^* D^*} = 7.7, \quad (20)$$

which deviate slightly from the SU(4) relations shown in Eq. (7). For the four-point coupling constants, there is no empirical information and we thus use the SU(4) relations to determine their values in terms of the three-point coupling constants. They are

$$g_{\pi\psi DD^*} = g_{\pi DD^*} g_{\psi DD}, \quad g_{\rho\psi DD} = g_{\rho DD} g_{\psi DD}, \quad g_{\rho\psi D^* D^*} = g_{\rho D^* D^*} g_{\psi D^* D^*}. \quad (21)$$

All meson masses are taken from the particle data book. In particular, the rho meson mass is taken to be 770 MeV without considering its large width. To obtain analytical expressions for the cross sections so they can be directly imported into a computer code for numerical calculations, we have used the software package FORM [18] to contract all Lorentz indices in Eq.(17).

A. Without form factors

Fig. 2 shows the cross sections of J/ψ absorption by π and ρ mesons as functions of the CM energy \sqrt{s} of the two initial-state mesons. The cross section $\sigma_{\pi\psi}$, shown by the solid curve, includes contributions from both $\pi\psi \rightarrow D\bar{D}^*$ and $\pi\psi \rightarrow D^*\bar{D}$, which have same cross sections. It is seen that the three J/ψ absorption cross sections have very different energy dependence near the threshold energy, $\max(m_1 + m_2, m_3 + m_4)$. While $\sigma_{\pi\psi}$ increases monotonously with CM energy, the cross section for the process $\rho\psi \rightarrow D\bar{D}$ decreases rapidly with CM energy, and that for the process $\rho\psi \rightarrow D^*\bar{D}^*$ changes little with CM energy after an initial rapid increase near the threshold.

In Fig. 3, we show the thermal average of these cross sections in a hadronic matter at temperature T , which is given by

$$\langle \sigma v \rangle = \frac{\int_{z_0}^{\infty} dz [z^2 - (\alpha_1 + \alpha_2)^2] [z^2 - (\alpha_1 - \alpha_2)^2] K_1(z) \sigma(s = z^2 T^2)}{4\alpha_1 K_2(\alpha_1) \alpha_2 K_2(\alpha_2)}, \quad (22)$$

where $\alpha_i = m_i/T$ ($i = 1$ to 4), $z_0 = \max(\alpha_1 + \alpha_2, \alpha_3 + \alpha_4)$, K_n 's are modified Bessel functions, and v is the relative velocity of initial-state particles in their collinear frame, i.e.,

$$v = \frac{\sqrt{(k_1 \cdot k_2)^2 - m_1^2 m_2^2}}{E_1 E_2}. \quad (23)$$

We find that although $\langle \sigma_{\pi\psi} v \rangle$ increases with increasing temperature, $\langle \sigma_{\rho\psi} v \rangle$ varies only moderately with temperature. Actually, the contribution of the process $\rho\psi \rightarrow D\bar{D}$ to $\langle \sigma_{\rho\psi} v \rangle$ even decreases with temperature. These features can be understood from the energy dependence of the cross sections shown in Fig. 2 and the difference in their kinematic thresholds (i.e., $m_3 + m_4 - m_1 - m_2$), which are roughly 0.64, -0.14, and 0.15 GeV for the processes $\pi\psi \rightarrow D^*\bar{D}(D\bar{D}^*)$, $\rho\psi \rightarrow D\bar{D}$, and $\rho\psi \rightarrow D^*\bar{D}^*$, respectively. The process $\pi\psi \rightarrow D^*\bar{D}(D\bar{D}^*)$ has the highest threshold, while the process $\rho\psi \rightarrow D\bar{D}$ is exothermic and thus has no threshold. With a pion in the initial-state, the process $\pi\psi \rightarrow D^*\bar{D}(D\bar{D}^*)$ requires very energetic pions to overcome the high energy threshold and thus has a small thermal average $\langle \sigma_{\pi\psi} v \rangle$ at low temperature. Since at higher temperatures not only are there more energetic pions which are able to overcome the kinematic threshold but also the cross section for the process $\pi\psi \rightarrow D^*\bar{D}(D\bar{D}^*)$ increases with the CM energy as shown in Fig. 2, $\langle \sigma_{\pi\psi} v \rangle$ thus increases strongly with temperature. For the process $\rho\psi \rightarrow D\bar{D}$, on the other hand, its contribution to the thermal average $\langle \sigma_{\rho\psi} v \rangle$ decreases with temperature because with increasing temperature there are fewer rho mesons at low energy, which contribute the largest cross section. The contribution of the process $\rho\psi \rightarrow D^*\bar{D}^*$ to $\langle \sigma_{\rho\psi} v \rangle$ changes slowly with temperature as a result of both the small threshold and the fact that the cross section only weakly depends on the CM energy.

In Fig. 4 we show the total cross section for each process and also the partial contributions from the four-point, PPV, and VVV couplings. Our results from PPV couplings alone (dot-dashed curves) are identical to the results from Matinyan and Müller [15]. Inclusion of the VVV and four-point couplings increases $\sigma_{\pi\psi}$ by an order of magnitude. For the process $\rho\psi \rightarrow D\bar{D}$, the decrease of the cross section after including four-point couplings is due to their destructive interference with the PPV coupling terms. The process $\rho\psi \rightarrow D^*\bar{D}^*$ is entirely due to VVV and four-point couplings and is seen to have a much larger cross section than that for the process $\rho\psi \rightarrow D\bar{D}$. As a result, inclusion of the VVV and four-point couplings also significantly increases $\sigma_{\rho\psi}$.

Fig. 5 shows the thermal average of the total cross section for each process together with the partial ones from the three different couplings. Similar to the above findings on $\sigma_{\pi\psi}$ and $\sigma_{\rho\psi}$, both $\langle \sigma_{\pi\psi} v \rangle$ and $\langle \sigma_{\rho\psi} v \rangle$ have much larger values than those from Matinyan and Müller [15].

B. With form factors

To take into account the composite nature of hadrons, form factors need to be introduced at interaction vertices. Unfortunately, there are no empirical information on form factors involving charm mesons. We thus take form factors as the usual mono-pole form at the three-point t channel and u channel vertices, i.e.,

$$f_3 = \frac{\Lambda^2}{\Lambda^2 + \mathbf{q}^2}, \quad (24)$$

where Λ is a cutoff parameter, and \mathbf{q}^2 is the squared three momentum transfer in the CM frame, given by $(\mathbf{p}_1 - \mathbf{p}_3)_{\text{cm}}^2$ and $(\mathbf{p}_1 - \mathbf{p}_4)_{\text{cm}}^2$ for t and u channel vertices, respectively. We assume that the form factor at four-point vertices has the following form:

$$f_4 = \left(\frac{\Lambda_1^2}{\Lambda_1^2 + \bar{\mathbf{q}}^2} \right) \left(\frac{\Lambda_2^2}{\Lambda_2^2 + \bar{\mathbf{q}}^2} \right), \quad (25)$$

where Λ_1 and Λ_2 are the two different cutoff parameters at the three-point vertices present in the process with the same initial and final particles, and $\bar{\mathbf{q}}^2$ is the average value of the squared three momentum transfers for t and u channels,

$$\bar{\mathbf{q}}^2 = \frac{[(\mathbf{p}_1 - \mathbf{p}_3)^2 + (\mathbf{p}_1 - \mathbf{p}_4)^2]_{\text{cm}}}{2} = p_{i,\text{cm}}^2 + p_{f,\text{cm}}^2. \quad (26)$$

To study the uncertainties due to form factors, we use the same value for all cutoff parameters for simplicity, i.e.,

$$\Lambda_{\pi DD^*} = \Lambda_{\rho DD} = \Lambda_{\rho D^* D^*} = \Lambda_{\psi DD} = \Lambda_{\psi D^* D^*} \equiv \Lambda, \quad (27)$$

and choose Λ as either 1 or 2 GeV.

Fig. 6 shows the cross sections as functions of the CM energy without and with form factors. It is seen that form factors strongly suppress the cross sections and thus cause large uncertainties in their values. However, the J/ψ absorption cross sections remain appreciable after including form factors at interaction vertices. As in Fig. 4, the process $\rho\psi \rightarrow D^* \bar{D}^*$ is still more important than the process $\rho\psi \rightarrow D \bar{D}$. The thermal average of J/ψ absorption cross sections with and without form factor is shown in Fig. 7. At the temperature of 150 MeV, $\langle \sigma_{\pi\psi v} \rangle$ and $\langle \sigma_{\rho\psi v} \rangle$ are on the order of 1 mb and 2 mb, respectively, which are comparable to those used in phenomenological studies of J/ψ absorption by co-moving hadrons in relativistic heavy ion collisions.

IV. DISCUSSIONS AND SUMMARY

In our study, the effective Lagrangian shown in Eq. (5) is obtained from applying the minimal substitution of Eq.(2) to the free Lagrangian. The resulting PPV, VVV, and four-point (PPVV and VVVV) interaction Lagrangians in Eq. (5) are exactly the same as those in the chiral Lagrangian approach [19]. They are, however, different from those used by Haglin [16] in which the effective Lagrangian is generated from Eq.(1) simply by

$$\partial_\mu \rightarrow \partial_\mu - igV_\mu. \quad (28)$$

This does not give a gauge-invariant Lagrangian, and the resulting scattering amplitude fails to conserve the current. The basic reason is that both pseudoscalar and vector mesons in SU(4) are represented by 4×4 matrices and thus do not commute, so the substitution shown in Eq. (28) does not correctly generate all interaction terms.

Values of the J/ψ absorption cross sections by hadrons obtained in our model with form factors are comparable to those from Martins, Blaschke and Quack [12], Haglin [16], and Wong, Barnes and Swanson [13], but are much larger than those from Kharzeev and Satz [14], and Matinyan and Müller [15]. The difference between our approach and Haglin's approach has been discussed above. As shown in Fig. 4 and Fig. 5, our results without form factors are much larger than those from Matinyan and Müller [15] because the latter only included pseudoscalar-pseudoscalar-vector-meson couplings. As to the energy dependence of J/ψ absorption cross sections, our results shown in Fig. 2 and Fig. 4 for the case without form factors are similar to those from Matinyan and Müller [15], and Haglin [16], which are also based on effective hadronic Lagrangians. Including form factors weakens the energy dependence of the absorption cross sections as shown in Fig. 6. However, the decrease of the absorption cross sections with energy is still not as fast as in the quark-exchange models [12,13]. This difference could be due to the fact that meson interactions in our effective hadronic Lagrangian approach involve derivative couplings, leading thus to a strong momentum dependence in the matrix elements, while the non-relativistic potential used in the quark-exchange model does not have an explicit momentum dependence. Including the relativistic corrections to the quark-quark potential will be useful for further studying the energy dependence of the J/ψ absorption cross sections in the quark-exchange model.

Form factors involving charm mesons introduce significant uncertainties to our model based on hadronic effective Lagrangians, because there is little experimental information available. Four-point vertices appear in all processes in our study. If all vector mesons are massless, it is possible to determine the form factor at a four-point vertex once form factors at three-point vertices are chosen [20]. This is achieved through the gauge invariance by requiring current conservation for the total amplitude that includes the form factors. Since the uncertainty of form factors involving charm mesons is already large for three-point vertices and the gauge invariance is only exact when all vector mesons are massless, we choose not to follow this more involved approach. Instead, we have shown the uncertainties due to form factors by using two different values for the cutoff parameters.

We have used the centroid value for the ρ meson mass in this study. Since the ρ meson width in vacuum is large (151 MeV), the threshold behavior of $\rho\psi$ processes may change with the ρ meson mass. E.g., a rho meson with mass below 630 MeV changes the process $\rho\psi \rightarrow D\bar{D}$ from exothermic to endothermic, and the energy dependence of the cross section near the threshold is thus changed from fast-decreasing (the dashed curve) shown in Fig. 2 to fast-rising (similar to the dot-dashed curve). On the other hand, a rho meson with mass above 920 MeV changes the process $\rho\psi \rightarrow D^*\bar{D}^*$ from endothermic to exothermic. We thus expect that the final value of the J/ψ absorption cross section by rho meson will be different once the ρ meson width is considered. However, the ρ meson spectral function is further modified in the hadronic matter produced in heavy ion collisions [21,22], so the effects of rho meson width on J/ψ absorption in hadronic matter are more involved. We therefore leave the effect of ρ meson width on charmonium absorption to a future study.

Finally, vector mesons are treated as gauge particles in our approach. Since the SU(4) symmetry is not exact, it is not clear to what extent they can be treated as gauge particles. An alternative approach [23] based on both the chiral symmetry and the heavy quark effective theory may be useful in understanding the meson-exchange model we have used here.

In summary, we have studied the J/ψ absorption cross sections by π and ρ mesons in a meson-exchange model that includes pseudoscalar-pseudoscalar-vector-meson couplings, three-vector-meson couplings, and four-point couplings. We find that these cross sections have much larger values than in a previous study, where only pseudoscalar-pseudoscalar-vector-meson couplings were included. Including form factors at the interaction vertices, we find that their thermal averages at the temperature of 150 MeV are on the order of 1 mb and 2 mb, respectively. These values are comparable to those used in phenomenological studies of J/ψ absorption in relativistic heavy ion collisions. Our results thus suggest that the absorption of J/ψ by co-moving hadrons may indeed play an important role in the observed suppression.

ACKNOWLEDGMENTS

We thank K. Haglin and C. Y. Wong for helpful communications. This work was supported in part by the National Science Foundation under Grant No. PHY-9870038, the Welch Foundation under Grant No. A-1358, and the Texas Advanced Research Program under Grant No. FY97-010366-068.

REFERENCES

- [1] T. Matsui and H. Satz, Phys. Lett. B **178**, 416 (1986).
- [2] M. C. Abreu *et al.*, the NA38 Collaboration, Z. Phys. C **38**, 117 (1988); C. Baglin *et al.*, Phys. Lett. B **220**, 471 (1989).
- [3] C. Baglin *et al.*, Phys. Lett. B **270**, 105 (1991); **345**, 617 (1995).
- [4] M. Gonin *et al.*, the NA50 Collaboration, Nucl. Phys. **A610**, 404c (1996); M. C. Abreu *et al.*, the NA50 Collaboration, Phys. Lett. B **450**, 456 (1999).
- [5] D. Kharzeev, C. Lourenço, M. Nardi, and H. Satz, Z. Phys. C **74**, 307 (1997).
- [6] See, e.g., R. Vogt, Phys. Rept. **310**, 197 (1999).
- [7] J.-P. Blaizot and J.-Y. Ollitrault, Phys. Rev. Lett. **77**, 1703 (1996).
- [8] C.-Y. Wong, Nucl. Phys. **A630**, 487 (1998).
- [9] W. Cassing and C. M. Ko, Phys. Lett. B **396**, 39 (1997); W. Cassing and E. L. Bratkovskaya, Nucl. Phys. **A623**, 570 (1997).
- [10] N. Armesto and A. Capella, Phys. Lett. B **430**, 23 (1998).
- [11] C. M. Ko, X.-N. Wang, B. Zhang, and X. F. Zhang, Phys. Lett. B **444**, 237 (1998).
- [12] K. Martins, D. Blaschke, and E. Quack, Phys. Rev. C **51**, 2723 (1995).
- [13] C.-Y. Wong, private communication.
- [14] D. Kharzeev and H. Satz, Phys. Lett. B **334**, 155 (1994).
- [15] S. G. Matinyan and B. Müller, Phys. Rev. C **58**, 2994 (1998). Note that some of our coupling constants are a factor of 2 smaller due to differences in the definitions.
- [16] K. Haglin, nucl-th/9907034.
- [17] Z. Lin, C. M. Ko, and B. Zhang, nucl-th/9905003, Phys. Rev. C., in press.
- [18] Made by J. Vermaseren, the free version of the software is available on the internet at <ftp://hep.itp.tuwien.ac.at/pub/Form/PC/>.
- [19] C. Song and V. Koch, Phys. Rev. C **55**, 3026 (1997). Before checking the similarity between our results and those in the chiral Lagrangian approach, one should take notice of the different normalizations for the coupling constant g and the meson matrices as well as the following typos in that paper. The first part of Eq.(A2) should be: $U = \exp\left[i\frac{\sqrt{2}}{f_\pi}\phi\right]$; Eq.(A3) should be: $D_\mu U = \partial_\mu U - igA_\mu^L U + igUA_\mu^R$; and the first part of Eq.(A5) should be: $\mathcal{L}_{V\phi\phi}^{(3)} = -\frac{ig}{2}\text{Tr}\partial_\mu\phi[V^\mu, \phi] + \dots$.
- [20] J. Kapusta, P. Lichard, and D. Seibert, Phys. Rev. D **44**, 2774 (1991); *ibid* **47**, 4171(E) (1993).
- [21] G. E. Brown and M. Rho, Phys. Rev. Lett. **66**, 2720 (1991); T. Hatsuda and S.H. Lee, Phys. Rev. C **46**, R34 (1992); M. Asakawa, C. M. Ko, P. Lévai, and X. J. Qiu, Phys. Rev. C **46**, R1159 (1992); C. M. Ko, V. Koch, and G. Q. Li, Ann. Rev. Nucl. Part. Sci. **47**, 505 (1997).
- [22] G. Agakishiev *et al.*, CERES Collaboration, Phys. Rev. Lett. **75**, 1272 (1995); P. Wurm *et al.*, CERES Collaboration, Nucl. Phys. **A590**, 103c (1995).
- [23] L.-H. Chan, Phys. Rev. D **55**, 5362 (1997).

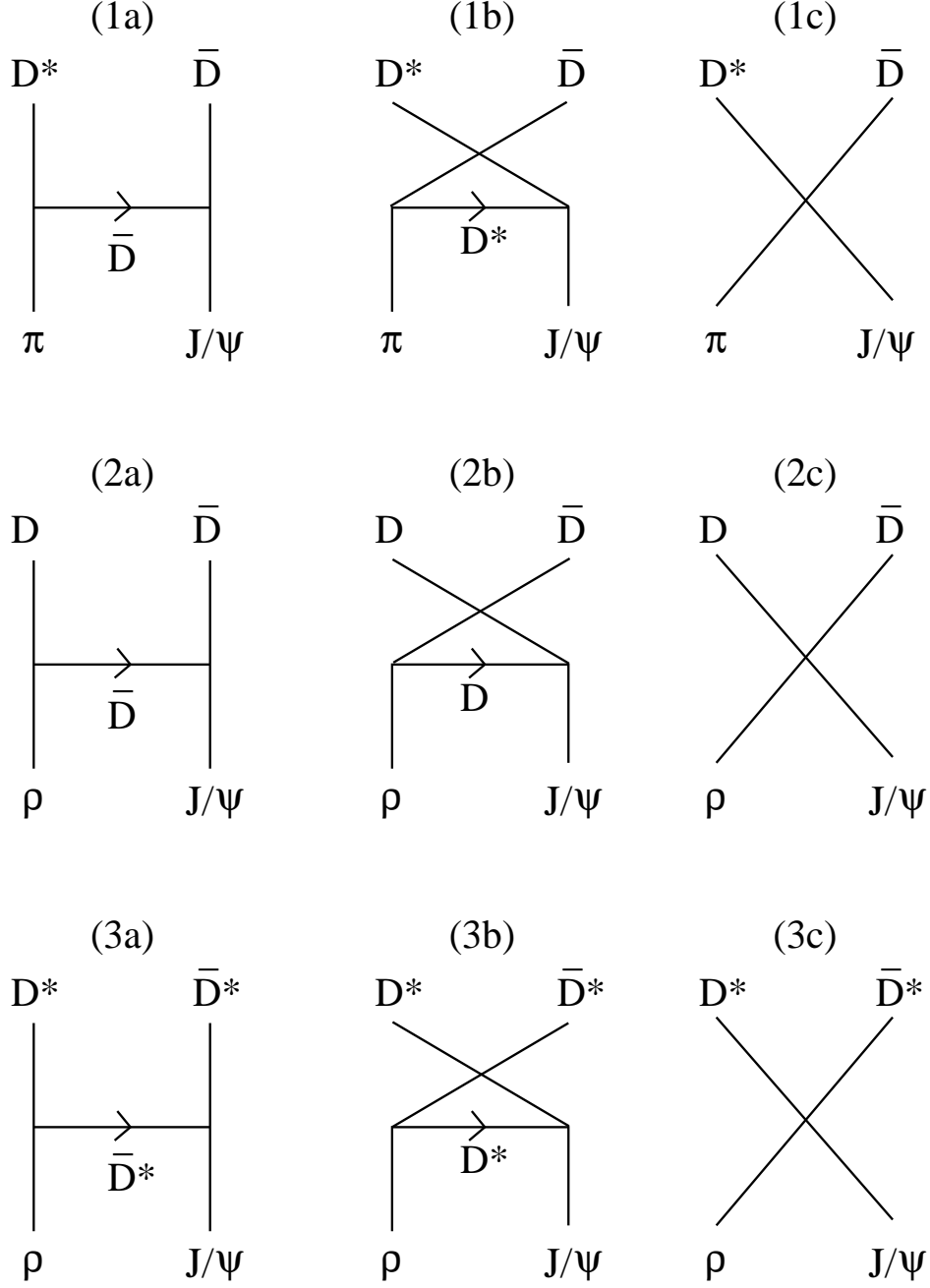


FIG. 1. Diagrams for J/ψ absorption processes. (1a-1c): $\pi\psi \rightarrow D^*\bar{D}$, (2a-2c): $\rho\psi \rightarrow D\bar{D}$, and (3a-3c): $\rho\psi \rightarrow D^*\bar{D}^*$. Diagrams for the process $\pi\psi \rightarrow D\bar{D}^*$ are similar to (1a)-(1c) but with each particle replaced by its anti-particle.

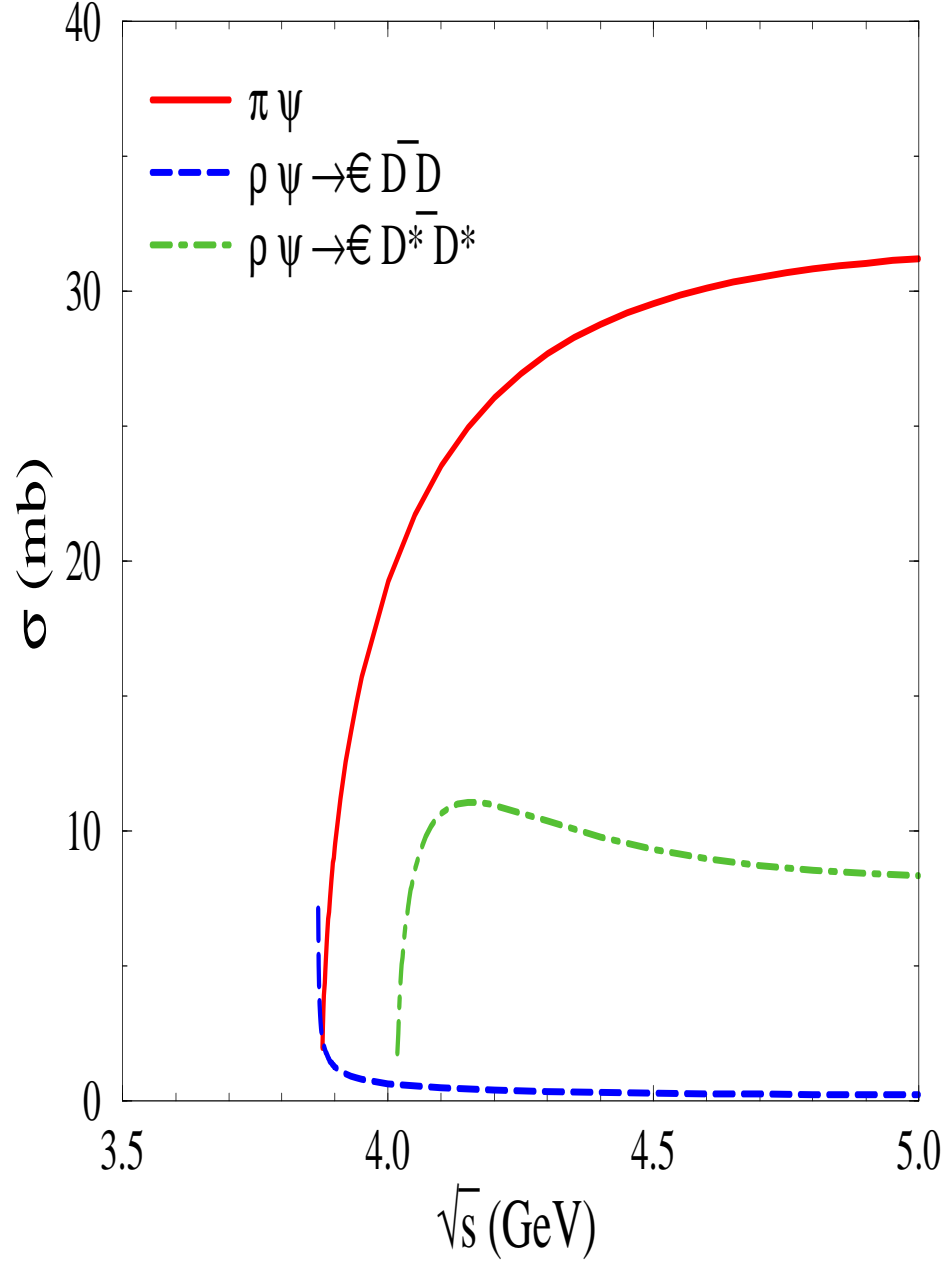


FIG. 2. J/ψ absorption cross sections (without form factors) as functions of the CM energy of initial-state mesons. The solid curve represents the total contribution from both $\pi\psi \rightarrow D^*\bar{D}$ and $\pi\psi \rightarrow \bar{D}^*D$ processes.

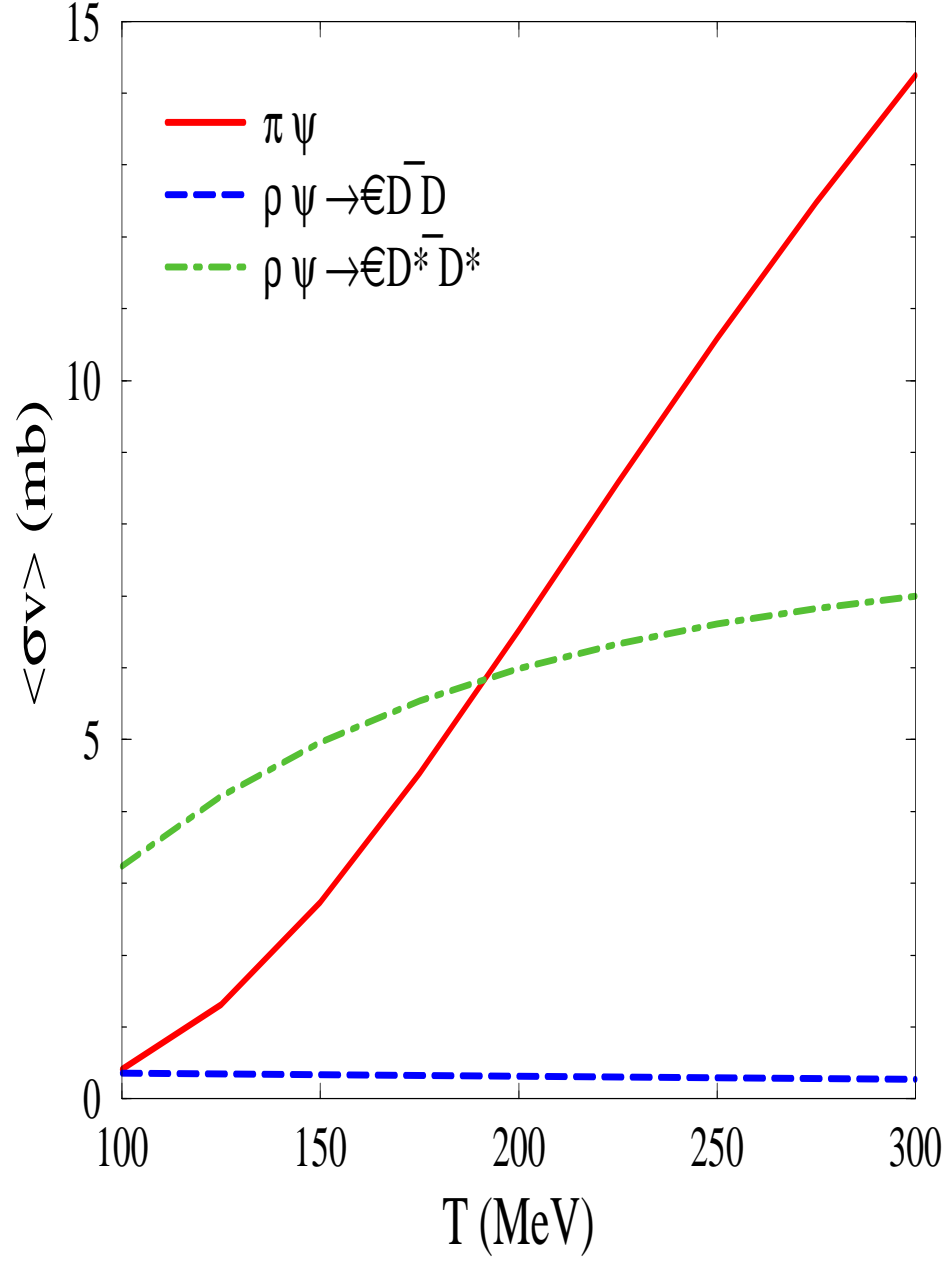


FIG. 3. Thermal average of J/ψ absorption cross sections (without form factors) as functions of temperature T .

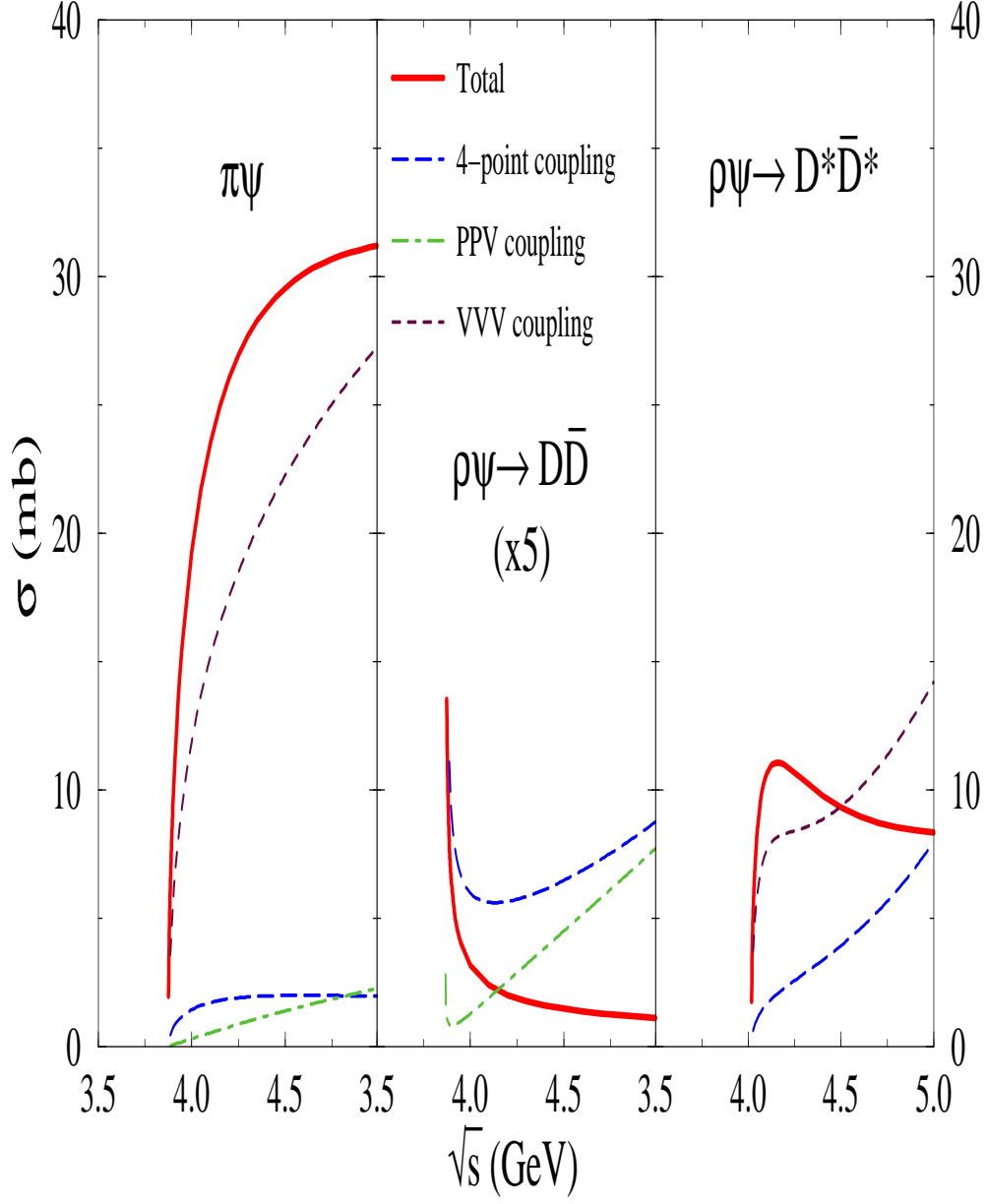


FIG. 4. Contributions from different couplings to J/ψ absorption cross sections (without form factors) as functions of the CM energy of initial-state mesons.

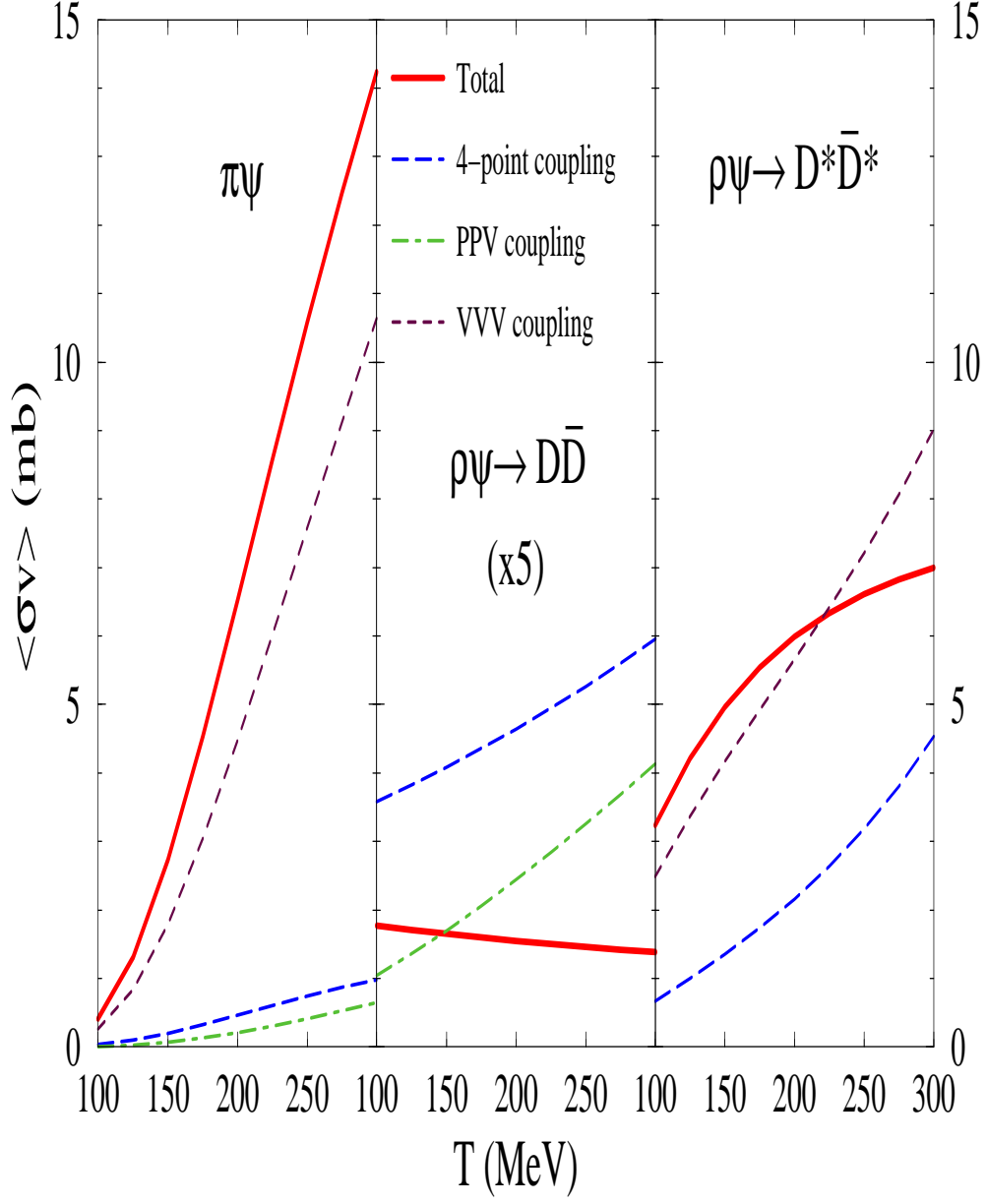


FIG. 5. Contributions from different couplings to the thermal average of J/ψ absorption cross sections (without form factors) as functions of temperature T .

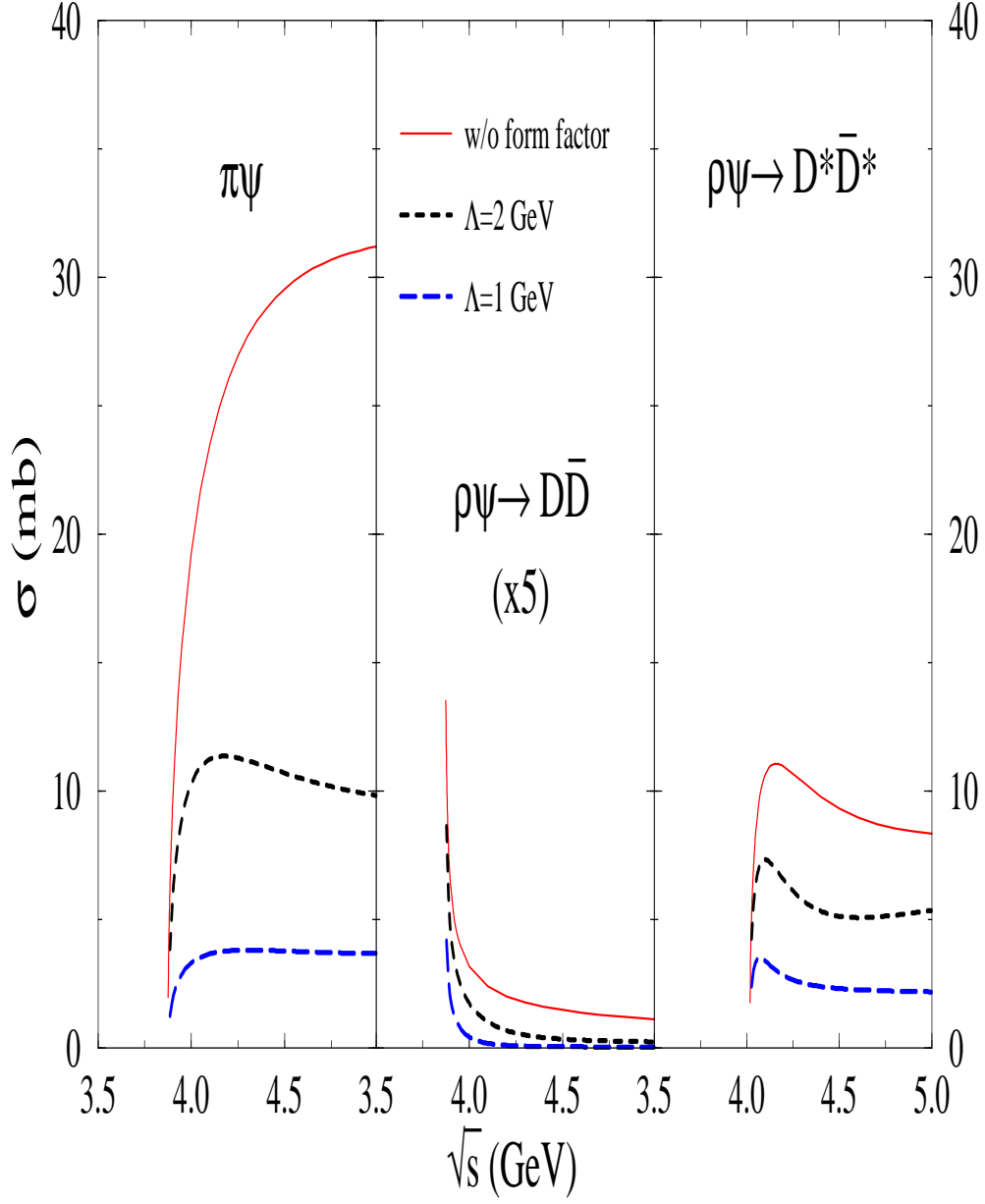


FIG. 6. Cross sections of J/ψ absorption as functions of the CM energy of initial-state mesons with and without form factors.

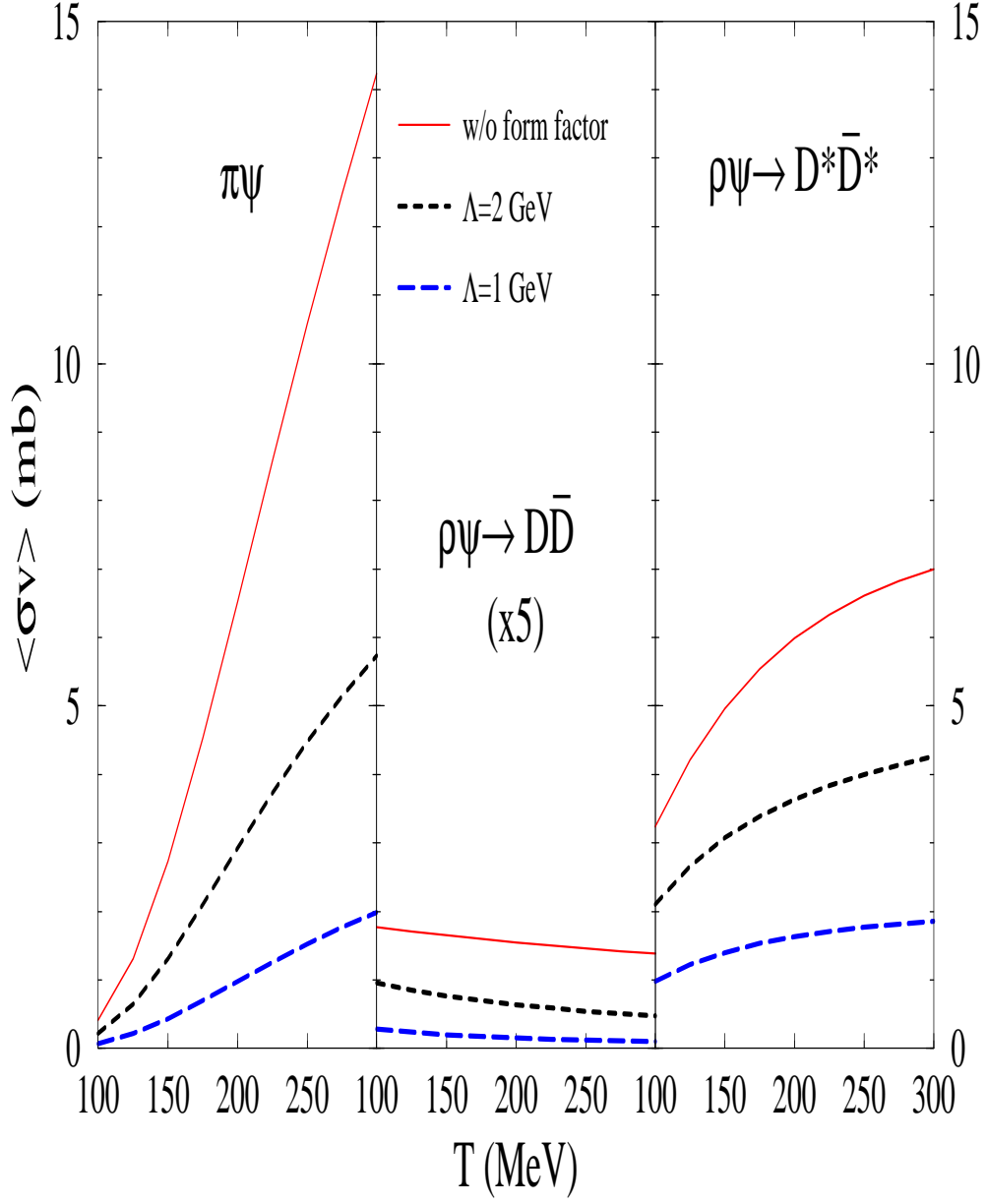


FIG. 7. Thermal-averaged cross sections of J/ψ absorption as functions of temperature T with and without form factors.